LA-12841-MS c.3

LA-12841-MS
c.3

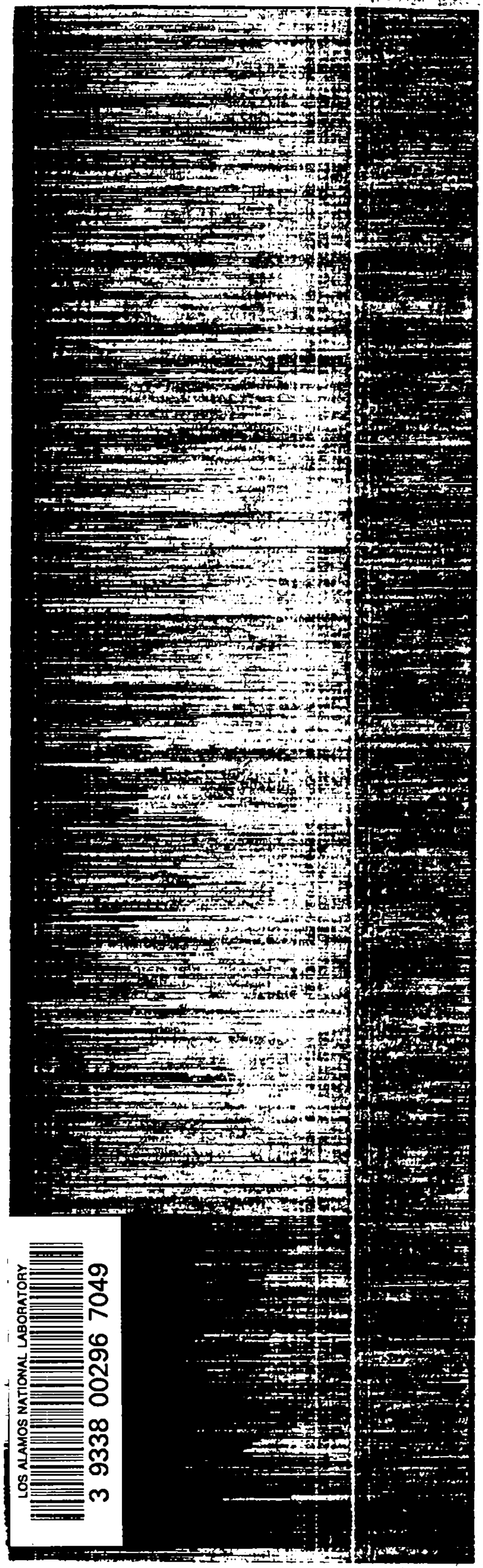

Global Equation of State for a Glassy Material: Fused Silica

Los Alamos
NATIONAL LABORATORY

Los Alamos National Laboratory is operated by the University of California for the United States Department of Energy under contract W-7405-ENG-36.

LA-12841-MS

UC-700
Issued: September 1994

Global Equation of State for a Glassy Material: Fused Silica

J. C. Boettger

Los Alamos
NATIONAL LABORATORY
Los Alamos, New Mexico 87545

GLOBAL EQUATION OF STATE FOR A GLASSY MATERIAL: FUSED SILICA

by

J. C. Boettger

ABSTRACT

A new SESAME equation of state (EOS) for fused silica has been generated using the computer program GRIZZLY and will be added to the SESAME library as material number 7387. This new EOS provides better agreement with experimental data than was achieved by all previous SESAME EOSs for fused silica. Material number 7387 also constitutes the most realistic SESAME-type EOS generated for any glassy material thus far.

I. INTRODUCTION

In recent years, considerable effort has been devoted to developing and refining techniques for accurately simulating shock-wave propagation through silicate materials (eg. quartz, granite, and rhyolite). This effort has been driven by the need to improve current capability to detect underground explosions, estimate their magnitudes, and discriminate between chemical and nuclear sources. One essential component of any such numerical simulation is a collection of realistic EOSs for all of the materials involved in the process being simulated. For this reason, there has been an ongoing effort to produce high quality SESAME-type[1] EOSs for various prototypical geologic materials[2-6] and to better understand the impact that EOS related properties have on wave propagation in silicates.

To date, there has been considerable success in this EOS effort. SESAME-type EOSs have been produced for the low- and high-pressure phases of crystalline quartz[4] and granite.[6] In addition, the single-phase granite EOSs have been shown to work well for rhyolite. Finally, a new dynamic phase mixing model has been developed[5] to describe the hysteretic structural phase transition exhibited by many silicate materials. In spite of these successes, there still are a number of important properties of shock-loaded silicates that cannot be adequately described during numerical simulations.

One of the more perplexing features of shock-loaded silicates is their tendency to release to a thermodynamic phase that is different from the initial phase. For example, it has been shown that when crystalline quartz (normal density $\rho_0 = 2.65$ gm/cc) is subjected to a peak stress of about 25-35 GPa, whether by hydrostatic loading or shock loading, the sample irreversibly transforms to a fused (glassy) silica with a density of about 2.2 gm/cc.[7,8] Similarly, if fused silica is loaded to stresses in the range of about 10-30 GPa, it irreversibly transforms to a densified silica glass with a density of about 2.4 gm/cc.[9,10] However, for peak stresses below 10 GPa or above 30 GPa, fused silica returns to its normal low-density glassy phase. Any truly predictive numerical simulation of wave propagation in silicates must be able to account for this rather drastic form of hysteresis.

In the current investigation, a new SESAME-type EOS has been generated for fused silica and has been added to the SESAME library as material number 7387. This new EOS has been carefully designed to be thermodynamically consistent with the existing single-phase SESAME EOSs for crystalline silica,[4] so that it can be used to model shock-induced transitions between the crystalline and amorphous forms of silica. In addition, this work on fused silica is intended to act as a model for future work on various types of vitrified (glassy) silicates. Thus, great care has been devoted to accurately incorporating the rather unusual properties of fused silica that were ignored in previous SESAME EOSs for this substance.[2] In particular, besides the properties already discussed, the bulk modulus of fused quartz is known to exhibit an anomalous decrease for pressures up to 2.0 GPa, followed by a steady increase with pressure.[11,12]

In the next section, the models and input parameters used to generate material number 7387 are described in detail. The new SESAME EOS for fused silica is then presented and discussed in Section III.

II. METHODOLOGY

For most of the EOSs in the SESAME library, the pressure P, internal energy E, and Helmholtz free energy A are each divided into three distinct terms:

$$P(\rho,T) = P_s(\rho) + P_n(\rho,T) + P_e(\rho,T) \tag{1}$$

$$E(\rho,T) = E_s(\rho) + E_n(\rho,T) + E_e(\rho,T) \tag{2}$$

$$A(\rho,T) = A_s(\rho) + A_n(\rho,T) + A_e(\rho,T) \tag{3}$$

where ρ is the density and T is the temperature. The subscripts s, n, and e denote the contributions from the static lattice (i.e., frozen nuclei) cold curve (zero temperature isotherm), the nuclear motion, and the thermal electronic excitations, respectively.

Thus, it is possible to calculate (or update) each term independently using any desired model. Here, all three pieces of the EOS have been generated with GRIZZLY.[13]

In GRIZZLY, the only model currently available for calculating the thermal electronic contributions to the EOS is the well-known Thomas-Fermi-Dirac (TFD) model.[14] For the present case, the thermal electronic contributions were first generated for each constituent atom. Those monatomic thermal electronic EOSs were then combined via additive volume mixing[13] to form the total thermal electronic EOS for fused silica. This portion of the calculation requires the atomic numbers (Si - 14, O - 8) and the atomic masses (Si - 28.086, O - 15.999) for the two constituent atoms.[15]

The thermal nuclear contributions for fused silica were obtained with the CHARTJD nuclear model, which is closely related to the well-known CHARTD model.[16] In this model, the material is treated as a Debye-Gruneisen solid at low temperatures and as an ideal gas at high temperatures. The CHARTJD model smoothly switches between those two limits for temperatures near the melt line, which is obtained from the Lindemann law. In addition to the data already discussed, this part of the calculation requires ambient values for the density (ρ_0), the melt temperature (T_m), the Debye temperature (Θ_D), and the Gruneisen parameter (γ_0). The values used here for ρ_0 (2.204 gm/cc), T_m (1900 K), and γ_0 (0.65) were chosen to match the parameters used to generate material number 7386.[2] The value used here for Θ_D (495 K) was taken from Ref. 12. The density dependence of the Gruneisen parameter was taken from the CHARTD model.[16]

For modest compressions (≤ 2.15), the static lattice cold curve was obtained by removing thermal contributions from an input Hugoniot read in as a table of particle velocities (U_p) and shock velocities (U_s) chosen to ensure that the final EOS matches various types of experimental data; see Table 1. For $U_p < 1.0$ km/s, the input Hugoniot was used to match the bulk modulus vs. pressure curve of fused silica, up to 6 GPa.[11,12] For $U_p \geq 2.8$ km/s, the input Hugoniot was taken directly from measured Hugoniot data.[7,17-20] The remainder of the input Hugoniot (1.0 km/s $< U_p < 2.8$ km/s) could not be directly taken from Hugoniot data because there are major inconsistencies between the various sets of data in that reqion.[7,17-20] This difficulty was overcome by requiring the final EOS for fused silica to reproduce the hydrostatic amorphization transition pressure of α-quartz,[7,8] when the new EOS is combined with the existing single-phase SESAME EOS for α-quartz.[4] This condition proved sufficient to resolve the discrepancies between the sets of Hugoniot data.

Table 1: Input Hugoniot Points For Fused Silica

U_p (km/s)	U_s (km/s)	U_p (km/s)	U_s (km/s)
0.000	4.095	0.985	4.268
0.247	3.880	1.100	3.850
0.350	3.870	2.150	4.838
0.509	3.902	2.800	5.600
0.688	4.128	4.500	8.450
0.853	4.265		

For compressions greater than 2.15, the theoretical cold curve was required to smoothly extrapolate to a mixed TFD cold curve. In the expanded region ($\rho < \rho_0$), the cold curve was fitted with a generalized Lennard-Jones form[13] that was required to smoothly connect with the compressed part of the cold curve and to have the correct cohesive energy (E_c). The input cohesive energy (145.1 kcal/mole) was selected to ensure that the α-quartz phase is more stable than the fused silica phase under ambient conditions. In addition to the parameters already mentioned, the expanded lattice cold curve calculation requires a parameter FACLJ[13] (here 3.0) that controls the shape of the cold curve.

III. MATERIAL NUMBER 7387

Figure 1 shows the theoretical bulk modulus of fused silica as a function of pressure for SESAME material number 7387. The calculated bulk modulus has a value of 36.7 GPa at $P = 0.0$ GPa, decreases to about 29.2 GPa for $P = 2.2$ GPa, and then rises to about 42 GPa at $P = 6.0$ GPa. This result is in good agreement with the experimental bulk modulus vs. pressure curve for fused silica,[11,12] which begins at 37.1 GPa for $P = 0.0$ GPa, drops to about 30 GPa for $P = 2.0$ GPa, and then rises to about 40 GPa at $P = 6.0$ GPa. In contrast, all previous EOSs for fused silica in the SESAME library have bulk modulii that monotonically increase with pressure. Thus, the present SESAME EOS should be prefered for all applications that might be effected by the behavior of fused silica near ambient conditions.

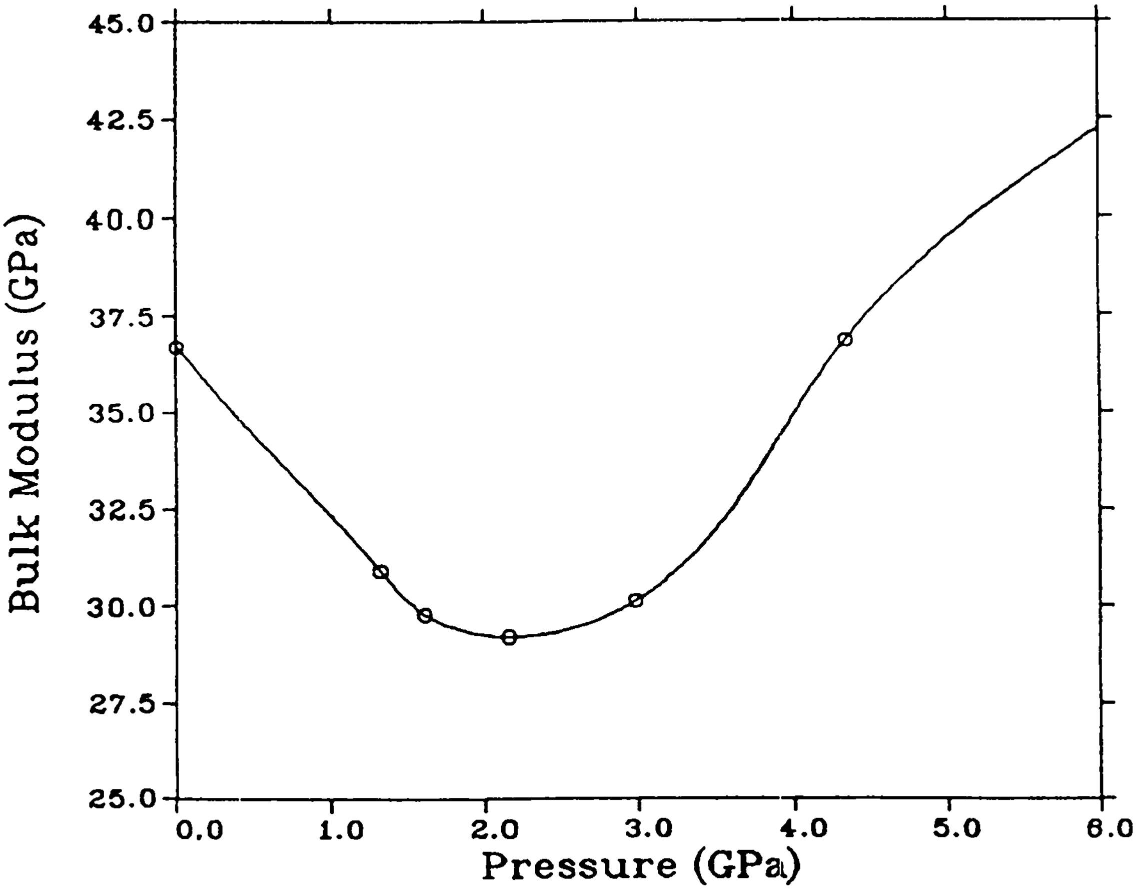

Figure 1. The theoretical bulk modulus of fused silica from SESAME material number 7387.

Figure 2 compares the present theoretical Hugoniot for fused silica with experimental data[7,17-20] and with the Hugoniot of the most recent prior SESAME EOS for fused silica, material number 7386.[2] For particle velocities less than about 2.2 km/s, the five sets of experimental data can be divided into two internally consistent groups, with the data from Refs. 7, 17, and 18 all lying well above the data from Refs. 19 and 20. The large disagreement between the two groups of data can be understood by considering the experimental techniques used. All of the higher U_s data were obtained from free surface velocity measurements using either the flash-gap technique or the wire-reflection technique. Both of these techniques require a number of assumptions to deduce the Hugoniot particle velocity and shock velocity from the free surface velocity. Unfortunately, the assumptions used in the necessary data analysis tend to be inadequate in regions of the Hugoniot where multiple waves are present. In contrast, the lower branch of the data in Figure 2 was obtained from time-resolved wave-profile measurements using either embedded particle velocity gauges[19] or velocity interferometry (VISAR) measurements.[20] Both of these latter two techniques are able to resolve multiple wave structures with great precision, and thus should be reliable in the region of interest.

As was discussed earlier, the branch of the Hugoniot data used during the generation of material number 7387 was determined by requiring the final EOS to reproduce the hydrostatic amorphization transition pressure for α-quartz. As can be seen in Fig. 2, this constraint produces a theoretical Hugoniot that lies just below the lower

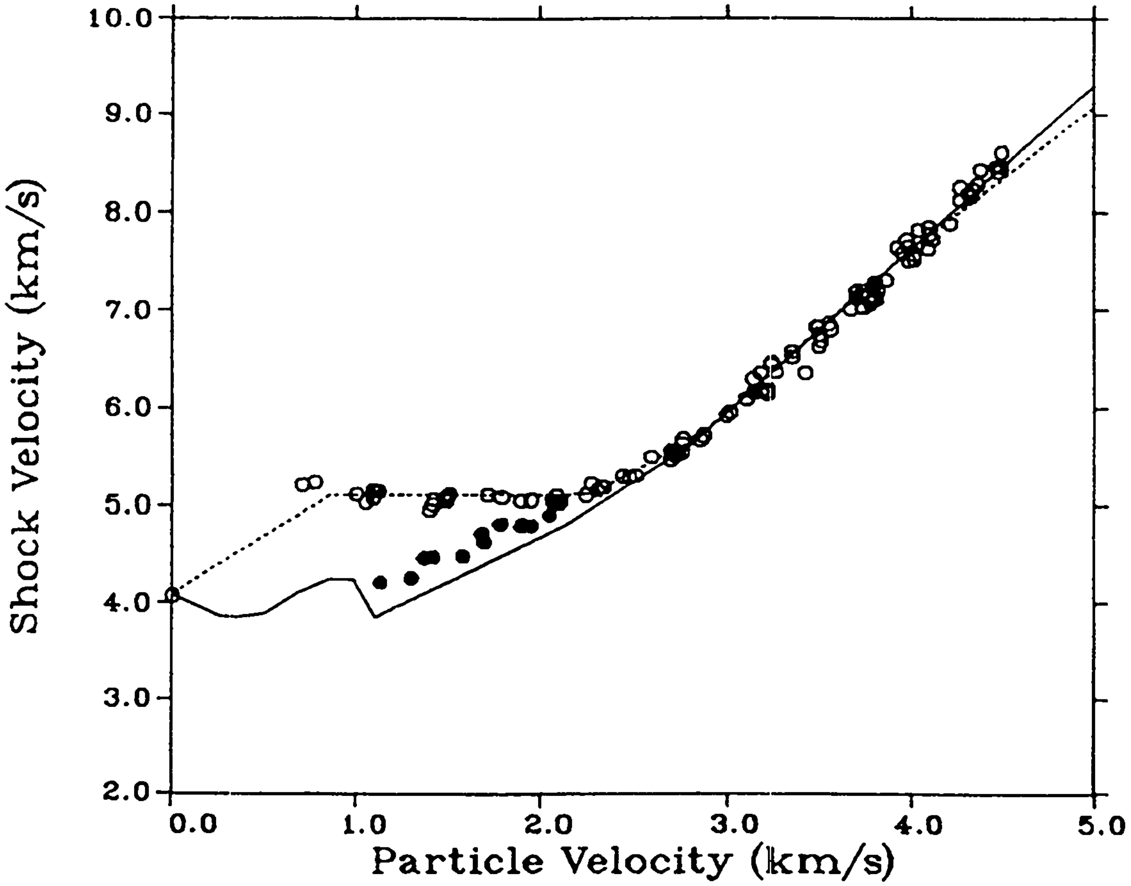

Figure 2. The theoretical Hugoniot for fused silica obtained from SESAME material number 7387 (solid line) is compared with experimental data from Refs 7, 17, and 18 (open circles) and Refs. 19 and 20 (solid circles). The theoretical Hugoniot for SESAME material number 7386 is also shown (dashed line).

branch of the data. This small difference between theory and experiment may be due to strength effects, which have not been included in the theoretical curve, or may be due to the rather large width of the plastic wave in the measured wave-profiles.[19,20] In both experiments, the shock state was determined by the mid-point of the plastic wave, while the theoretical Hugoniot should reflect the final state in the fused silica long after the shock wave has passed. The sharp drop in the theoretical Hugoniot at about U_p = 1.0 km/s corresponds to a stress of about 10 GPa and thus may reflect the observed densification transition.[9,10] The drop in the shock velocity should also produce a two-wave structure for particle velocities up to about 1.6 km/s, in good qualitative agreement with the time-resolved shock-wave data.[19] Overall, the fact that the new SESAME EOS for fused silica matches such a diverse collection of experimental data provides strong evidence that the lower branch of the Hugoniot data is in fact the correct one, as was suggested earlier.

The two theoretical Hugoniots in Figure 2 are substantially different for U_p < 2.2 km/s. This result is not surprising since the older EOS (material number 7386) was designed to fit the high U_s branch of the Hugoniot data and did not attempt to reproduce the anomalous bulk modulus of fused silica in the very low pressure region.[2] For these reasons, SESAME material number 7387 should be prefered over material number 7386 for all applications involving fused silica.

REFERENCES

1. S. P. Lyon and J. D. Johnson, editors, "SESAME: The Los Alamos National Laboratory Equation Of State Database," Los Alamos National Laboratory Document LA-UR-92-3407 (October 1992).
2. J. C. Boettger, "SESAME Equation Of State Number 7386, Fused Quartz," Los Alamos National Laboratory Report LA-11488-MS (January 1989).
3. J. C. Boettger and S. P. Lyon, "Method of Obtaining SESAME Equations Of State for Porous Materials: Application to Garnet Sand," Los Alamos National Laboratory Report LA-11726-MS (March 1990).
4. J. C. Boettger, "New Multiphase Equation of State for Polycrystalline Quartz," Los Alamos National Laboratory Report LA-11918-MS (October 1990).
5. J. C. Boettger, J. Appl. Phys. 72, 5500 (1992).
6. J. C. Boettger, "Multi-Phase Equation of State for Westerly Granite," Los Alamos National Laboratory Report LA-12470-MS (January 1993).
7. J. Wackerle, J. Appl. Phys. 33, 922 (1962).
8. R. J. Hemley, A. P. Jephcoat, H. K. Mao, I. C. Ming, and M. H. Manghnani, Nature 334, 52 (1988).
9. M. Grimsditch, Phys. Rev. Lett. 52, 2379 (1984).
10. R. J. Hemley, H. K. Mao, P. M. Bell, and B. O. Mysen, Phys. Rev. Lett. 57, 747 (1986).

11. T. Sasakura, K. Suito, and H. Fujisawa, Proc. of the XIth AIRAPT Int. Conf. on High Pressure Science and Technology - Kiev, edited by N. V. Novikov and Ye. M. Chistyakov, Vol. 2, pp. 60-72 (Naukova Dumka, 1989).

12. K. Suito, M. Miyoshi, T. Sasakura, and H. Fujisawa, *High-Pressure Research: Application To Earth And Planetary Sciences*, edited by Y. Syono and M. H. Manghnani (Terra Scientific Publishing, Tokyo, 1992), pp. 219-225.

13. Joseph Abdallah, Jr., "User's Manual for GRIZZLY," Los Alamos National Laboratory report LA-10244-M (September 1984).

14. R. D. Cowan and J. Ashkin, Phys. Rev. 105, 144 (1957).

15. N. W. Ashcroft and N. D. Mermin, *Solid State Physics* (Holt, Rinehart, and Winston, New York, 1976).

16. S. L. Thompson and H. S. Lawson, "Improvements to the CHART-D Radiation-Hydrodynamics Code III; Revised Analytic Equations of State," Sandia Laboratories report SC-RR-710714 (1972).

17. S. P. Marsh, editor, *LASL Shock Hugoniot Data* (U. C. Press, Berkeley, 1980).

18. R. G. Mcqueen, J. N. Fritz, and J. W. Hopson, Los Alamos National Laboratory document, M-6-200 (1985).

19. H. Sugiura, K. Kondo, and A. Sawaoka, J. Appl. Phys. 52, 3375 (1981).

20. L. C. Chhabildas and D. E. Grady, *Shock Waves In Condensed Matter*, edited by J. R. Asay, R. A. Graham, and G. K. Straub (Elsevier, Amsterdam, 1984), pp. 175-178.

Los Alamos
NATIONAL LABORATORY
Los Alamos, New Mexico 87545